VELOCITY MEASUREMENTS AND CONCENTRATION FIELD VISUALIZATIONS IN NATURAL CONVECTION COPPER ELECTROLYSIS UNDER MAGNETIC FIELD INFLUENCE

T. Weier, J. Hüller, G. Gerbeth, F.–P. Weiss

Forschungszentrum Rossendorf, P.O. Box 51 01 19, 01314 Dresden, Germany
(T.Weier@fz-rossendorf.de)

Introduction. Magnetic fields might have a manifold of influences on electrochemical reactions, including but not limited to the alteration of fluid properties, electrode reaction kinetics and morphology of surface deposits. For a recent review on the subject see [1]. However, the most prominent effect of the magnetic field is that on the transport of electroactive species. The influence of Lorentz force (LF) induced convection on mass transfer is well recognized since a long time. Several equations to describe the dependence of the limiting current density j_l on the applied magnetic induction B_0 have been proposed based on modeling and experimental data, see e.g. [2, 3, 4, 5]. If one assumes a power law relation of the type $j_l \sim B_0^m$, values of $m = 1/3$ and $m = 1/2$ seem widely accepted, nevertheless [6] report a considerable spread $0.25 < m < 1.64$ of measured exponents. Presumably, the reason for these discrepancies can be found in different field configurations and cell geometries and therefore a wide range of flow configurations. For a better understanding of those relations it would be desirable to study the LF induced motion directly. However, corresponding attempts reported in the literature are limited to flow visualizations (e.g. [7]) and interferometry of laminar flows in very small cells (e.g. [8]). The aim of the present study is to demonstrate that velocity measurements can provide valuable information for the interpretation of limiting current measurements under magnetic field influence.

1. Experimental setup. A small electrolytic cell with inner dimensions as given in Fig. 1 was made from PMMA. The side walls forming the electrodes consist of 0.5 mm thick copper plates. Neodymium–Iron–Boron permanent magnets 30 mm × 10 mm wide in x and y–direction and 6 mm extension in z, i.e the magnetization direction, are fixed behind the electrodes and used to provide a static magnetic field mainly oriented in z–direction. Its measured decay with in-

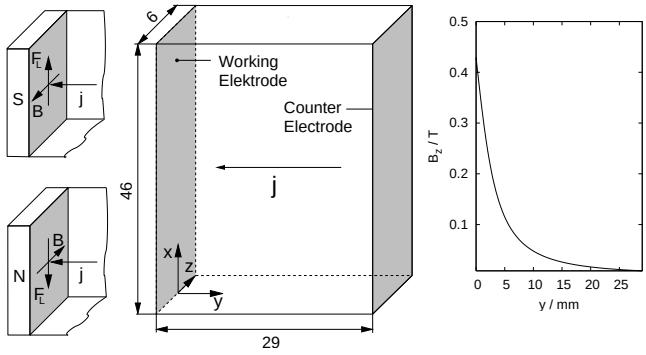

Fig. 1. Sketch of the electrolytic cell and the field configurations near the electrode (left). Decay of B_z with the distance from the electrode (right).

creasing distance from the electrode surface is given in the right part of Fig. 1. In all experiments, the lower edge of the magnets coincided with the lower edge of the cell. Since the LF is given by the vector product of current density **j** and magnetic induction **B**, it follows that a current density in y–direction and a magnetic induction in z–direction will generate a LF with an x–component only. The direction of this LF (upwards or downwards) depends on the electrical current and the orientation of the magnet as sketched in the left part of Fig. 1.

The chemical reaction under investigation was $Cu^{2+} + 2\ e^- \rightleftharpoons Cu$. Three different concentrations of $CuSO_4$ (0.1, 0.2, and 0.375 M) in an aqueous 1.5 M H_2SO_4 solution have been used during the experiments. Copper is deposited at the working electrode (WE) at a potential of -400 mV versus Pt_{RE}. This potential has been found sufficient to guarantee limiting current conditions for copper deposition under all concentrations and field configurations used.

Qualitative information on the concentration distribution in the cell was obtained by a shadowgraph technique. It visualizes the second spatial derivative of the density. Velocity fields in the x–y–plane were measured using a simple Digital Particle Image Velocimetry (DPIV) as described in [9] and [10].

2. Results and discussion. The left diagram in Fig. 2 shows the response of the cell current for a 0.1 M $CuSO_4$ solution to the potential step from the rest potential to -400 mV versus Pt_{RE} at the WE. The copper deposition caused by the potential change leads to a decrease of the Cu^{2+} concentration near the WE. Correspondingly copper dissolves at the counter electrode (CE), leading to a denser solution there. The density differences give rise to a natural convection directed upwards (positive x–direction) at the WE and downwards at the CE. After a certain time, steady state limiting current conditions are reached. The limiting current amounts to $j_l = 42.4\,\mathrm{Am}^{-2}$ in the absence of a magnetic field. A downwards directed LF increases this value to $j_l \approx 53.4\,\mathrm{Am}^{-2}$ while a magnetic field of the same strength but opposite direction producing an LF pointing upwards leads to the markedly higher value of $j_l \approx 69.4\,\mathrm{Am}^{-2}$. In case of the upwards directed LF the chronoamperogram in Fig. 2 displays a local minimum at $t \approx 25 \ldots 60$ s with $j_l \approx 62.8\,\mathrm{Am}^{-2}$. This minimum corresponds to a minimum of the measured x–component of the mean velocity ($\bar{u}$) in the near-electrode region.

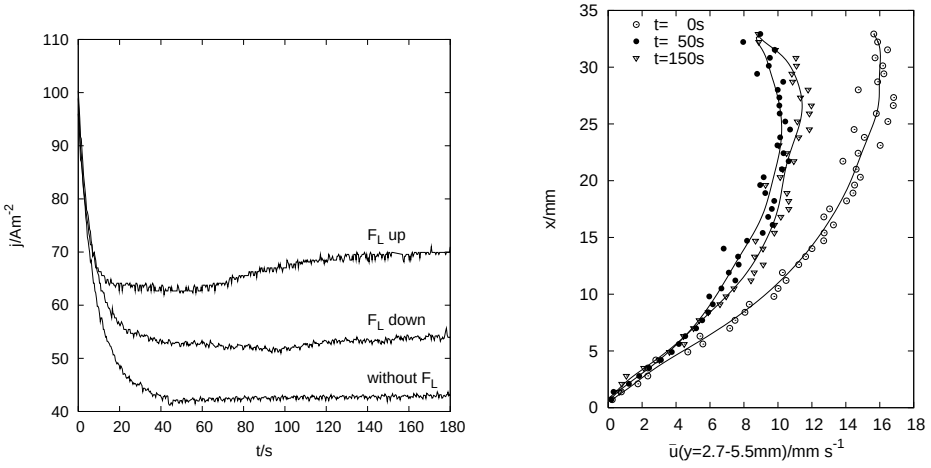

Fig. 2. Chronoamperometry for different LF configurations at the WE (left) and x–component of the velocity near the WE (averaged over y=2.7,. . . ,5.5 mm) for an upwards directed LF (right) in 0.1 M $CuSO_4$.

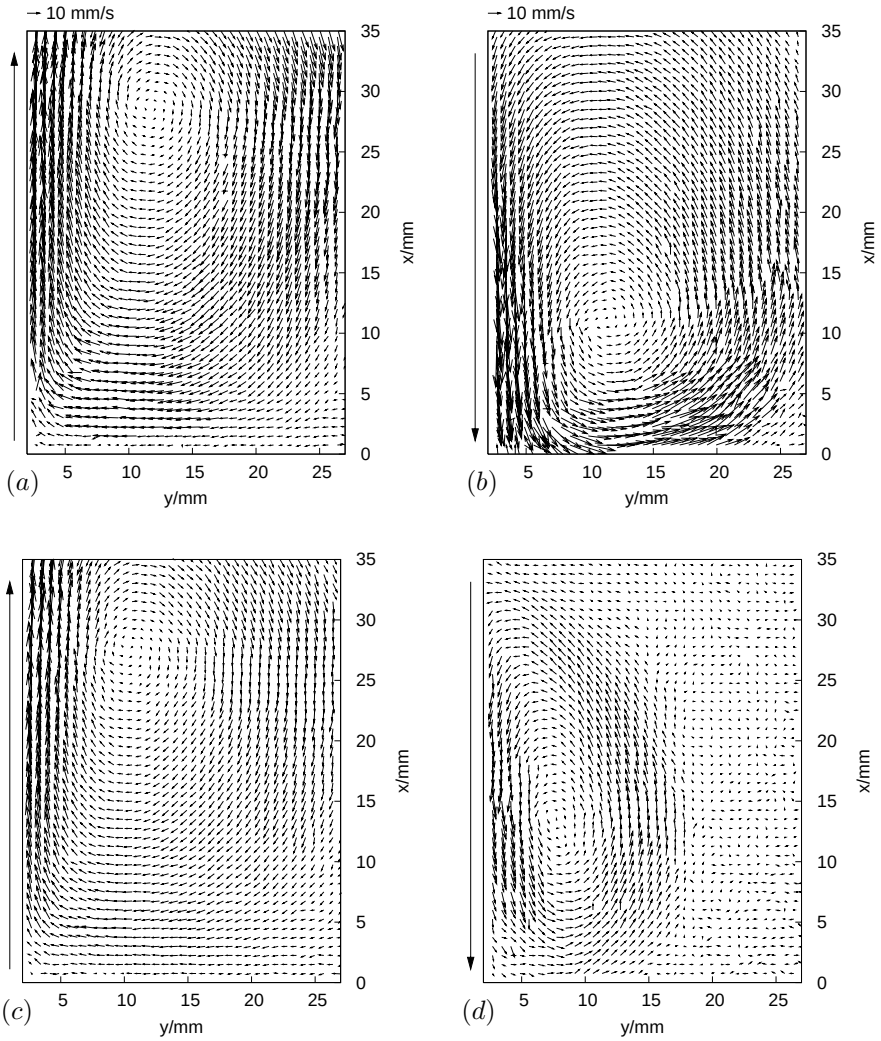

Fig. 3. Velocity fields for the 0.1 M $CuSO_4$ solution at $t = 0\,\mathrm{s}$ (a, b) and $t = 150\,\mathrm{s}$ (c, d) for upwards (a, c) and downwards (b, d) LF at WE.

Velocity fields in the cell measured by DPIV are shown in Fig. 3. The subfigures (a) and (b) give the velocity distribution immediately after the potential step. In both cases, the relatively high current densities result in pronounced vortex structures in the whole cell. In case of an upward directed LF (Fig. 3*a*, the fluid moves in clockwise direction around a center in the upper left part of the cell. For the downward directed LF (Fig. 3*b*), the motion is counterclockwise and the vortex center is in the lower left part of the cell. Despite the different directions of rotation, both velocity fields are rather similar (note that the measured region omits a part of the upper cell region and does not extend directly to the cell walls). The maximum velocity found at $t = 0\,\mathrm{s}$ for a downward LF is 22 mm/s, for the upwards directed force it is only slightly higher with 23 mm/s. Under steady state conditions ($t = 150\,\mathrm{s}$) the picture changes. While the upward force (Fig. 3c) still maintains a dominant single vortex flow in the whole cell, the vortex due to the downward directed LF is much smaller. Likewise, the maximum velocities differ now considerably, 15.3 mm/s for upward versus 8.2 mm/s for downward forcing. The differences in the velocity magnitudes explain the differences in the limiting current density measurements shown in Fig. 2.

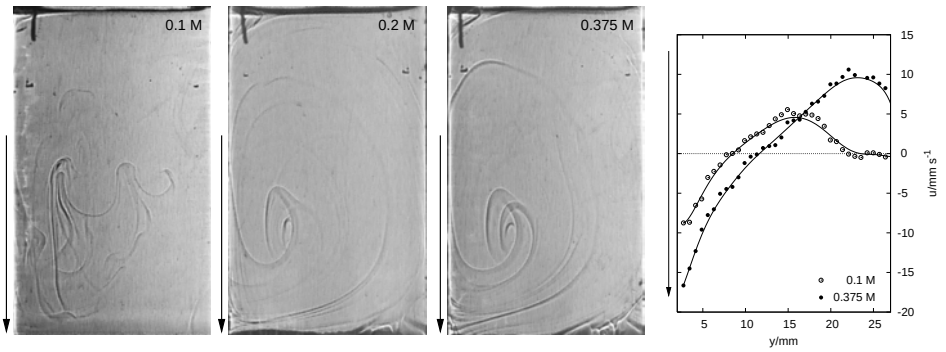

Fig. 4. Shadowgraph images 70 s after the potential step for a downward directed LF (arrow) at the WE and different $CuSO_4$ concentrations (left). x–component of the velocity in a horizontal cut at $x = 22$ mm (right).

In Fig. 4 shadowgraph images are shown for three different $CuSO_4$ concentrations and a downwards directed LF at the WE, 70 s after the potential step has been applied. For the 0.1 M $CuSO_4$ solution, the shadowgraph shows wave like structures in the lower region of the electrode. In the middle part of the cell plumes rise upwards. The LF is able to drive the lighter near–cathode fluid downwards. However, since the magnetic field and thereby the LF decay with the distance from the electrode, the situation is highly unstable. As soon as the lighter fluid moves away from the cathode, buoyancy seems to be able to counteract the LF and drives the fluid upwards. The picture changes for the 0.2 M $CuSO_4$ solution. Due to the higher bulk concentration, the limiting current density is larger ($j_l = 71.0\,\mathrm{Am}^{-2}$ for the case without magnetic field) compared to the 0.1 M solution. Consequently, a larger LF will be generated. On the other hand, buoyancy is increased as well, since the density difference between the Cu^{2+} free solution and the bulk increases. However, the LF obviously dominates the flow. A regular vortex structure with a center in the lower left part of the cell, where the driving force is maximum, is formed. Recirculation regions in the top left and lower right corner of the cell can be deduced. A similar flow structure evolves for the 0.375 M $CuSO_4$ solution. The velocity measurements given in the right diagram of Fig. 4 correspond to the visual impressions. While the fluid in the left part of the cell is almost stagnant for the 0.1 M solution and the overall velocities are low, convection with comparable high velocities dominates the whole cell in case of the 0.375 M solution.

REFERENCES

1. T. Z. Fahidy. The effect of magnetic fields on electrochemical processes. In B. E. Conway, editor, *Modern Aspects of Electrochemistry*, no. 32 (Kluwer/Plenum, New York, 1999) pp. 333–354.
2. R. Aogaki, K. Fueki, T. Mukaibo. *Denki Kagaku*, vol. 43 (1975), no. 9, pp. 509–514.
3. O. Aaboubi, *et al.* *J. Electrochem. Soc.*, vol. 137 (1990), no. 6, pp. 1796–1804.
4. N. Leventis, *et al.* *J. Phys. Chem. B*, vol. 102 (1998), pp. 3512–3522.
5. B. Fricoteaux, B. Jonvel, J.-P. Chopart. *J. Phys. Chem. B*, vol. 107 (2003), pp. 9459–9464.
6. K. Kim, T. Fahidy. *J. Electrochem. Soc.*, vol. 142 (1995), no. 12, pp. 4196–4204.
7. Z. Gu, T. Fahidy. *J. Electrochem. Soc.*, vol. 134 (1987), no. 4, pp. 2241–2248.
8. R. O'Brien, K. Santhanam. *J. Electrochem. Soc.*, vol. 129 (1982), no. 6, pp. 1266–1268.
9. C. Willert, M. Gharib. *Experiments in Fluids*, vol. 10 (1991), pp. 181–193.
10. L. Gui, W. Merzkirch. *Experiments in Fluids*, vol. 28 (2000), pp. 36–44.